Cite as: Cui *et al.*, *Science* 10.1126/science.aaf2458 (2016).

Pore chemistry and size control in hybrid porous materials for acetylene capture from ethylene

Xili Cui,[1]* Kaijie Chen,[2]* Huabin Xing,[1]† Qiwei Yang,[1] Rajamani Krishna,[3] Zongbi Bao,[1] Hui Wu,[4] Wei Zhou,[4] Xinglong Dong,[5] Yu Han,[5] Bin Li,[6] Qilong Ren,[1] Michael J. Zaworotko,[2]† Banglin Chen[6]†

[1]Key Laboratory of Biomass Chemical Engineering of Ministry of Education, College of Chemical and Biological Engineering, Zhejiang University, Hangzhou 310027, China. [2]Department of Chemical and Environmental Sciences, University of Limerick, Limerick, Republic of Ireland. [3]Van't Hoff Institute for Molecular Sciences, University of Amsterdam, Science Park 904, 1098 XH Amsterdam, Netherlands. [4]Center for Neutron Research, National Institute of Standards and Technology, Gaithersburg, MD 20899-6102, USA. [5]Advanced Membranes and Porous Materials Center, Physical Sciences and Engineering Division, King Abdullah University of Science and Technology, Thuwal 23955-6900, Saudi Arabia. [6]Department of Chemistry, University of Texas–San Antonio, One UTSA Circle, San Antonio, TX 78249-0698, USA.

*These authors contributed equally to this work.

†Corresponding author. Email: xinghb@zju.edu.cn (H.X.); michael.zaworotko@ul.ie (M.J.Z.); banglin.chen@utsa.edu (B.C.)

The trade-off between physical adsorption capacity and selectivity of porous materials is a major barrier for efficient gas separation and purification through physisorption. We report control over pore chemistry and size in copper coordination networks with SiF_6^{2-} and organic linkers for the preferential binding and orderly assembly of acetylene molecules through cooperative host-guest and/or guest-guest interactions. The specific binding sites for acetylene are validated by modeling and neutron powder diffraction studies. The energies associated with these binding interactions afford high adsorption capacity (2.1 mmol/g at 0.025 bar) and selectivity (39.7 to 44.8) for acetylene at ambient conditions. Their efficiency for the separation of acetylene/ethylene mixtures is demonstrated by experimental breakthrough curves (0.73 mmol/g from 1/99 mixture).

An urgent demand for efficient solutions to challenges in gas separations, sensing and storage (*1*–*7*) has spurred research on custom-designed porous materials, termed as metal-organic frameworks (MOFs) and/or porous coordination polymers (PCPs) (*8*), in which open lattices are formed from inorganic centers (nodes) and organic linking groups. These materials can be designed from first principles and, thanks to their inherent diversity, afford exquisite control over pore chemistry and pore size.

Ideal porous materials for gas separation should exhibit high selectivity and optimal adsorption capacity for the target gas molecules at relevant conditions. However, the design of new materials that improve upon existing benchmarks, poses a daunting challenge to materials scientists (*9*–*12*). For example, porous materials are needed for acetylene (C_2H_2) capture and separation from ethylene (C_2H_4) (*13*–*17*), industrial processes relevant for the production of polymer-grade C_2H_2 and C_2H_4 (the most produced organic compound in the world, over 140 million tons/year in 2014). The MOF-74 family of compounds exhibits a high density of open metal sites that drive high uptake of C_2H_2 but display low separation selectivities (*18*). The M'MOFs family exhibits ultramicropores that enable sieving effects and the high separation selectivities, but relatively low uptake of C_2H_2 (*19*).

We report that coordination networks comprised of preformed inorganic (hexafluorosilicate, SiF_6^{2-}, SIFSIX) and organic linkers, SIFSIX-2-Cu-i (2 = 4,4'-dipyridylacetylene, i = interpenetrated) (*20*) and SIFSIX-1-Cu (1 = 4,4'-bipyridine) (*21*), can exhibit exceptional C_2H_2 capture performance because the geometric disposition of SiF_6^{2-} moieties enables preferential binding of C_2H_2 molecules. Both materials exhibit pore spaces that enable extremely high C_2H_2 capture under low pressures and unexpectedly afford new benchmarks for the highly efficient removal of minor amounts of C_2H_2 from C_2H_4 gas and mass separation of C_2H_2 /C_2H_4 mixtures under ambient conditions, respectively. We attribute this unprecedented performance to the existence of sweet-spots in pore chemistry and pore size that enable highly specific recognition of C_2H_2 and high uptake to occur in the same material.

In these "SIFSIX" materials, two-dimensional (2D) nets of organic ligand and metal node are pillared with SiF_6^- anions in the third dimension to form 3D coordination networks that exhibit primitive cubic topology and, importantly, pore walls lined by inorganic anions (*20*–*23*). The pore sizes within this family of materials can be systematically tuned by changing the length of the organic linkers, the metal node and/or framework interpenetration. SIFSIX-1-Cu, SIFSIX-2-Cu, SIFSIX-2-Cu-i, SIFSIX-3-Cu (3 = pyrazine), SIFSIX-3-Zn, and SIFSIX-3-Ni have already been studied for their exceptional CO_2 capture performance but herein we report a study of their C_2H_2 and C_2H_4 adsorption from 283 to 303 K. Figure 1, A and B, and figs. S2 to S7 (*24*)

reveal dramatically different adsorption behaviors toward C_2H_2 than observed for CO_2 (figs. S8 and S9) (*24*). SIFSIX-2-Cu-i rapidly adsorbs C_2H_2 at very low pressure (≤ 0.05 bar). Indeed, its C_2H_2 uptake reaches 2.1 mmol/g at 298 K and 0.025 bar (Fig. 1B) versus 1.78 mmol/g on UTSA-100a (*17*). This performance at low pressures indicates that SIFSIX-2-Cu-i offers promise for C_2H_2 capture when it is a minor component in a gas mixture. SIFSIX-1-Cu exhibits extraordinary C_2H_2 uptake (8.5 mmol/g) at 298 K and 1 bar. This is not only the highest uptake of SIFSIX materials, but is even higher than the previous benchmark, FeMOF-74 (table S1) (*18*, *24*). As detailed herein we attribute the unprecedented performance of these materials to their hybrid pore chemistry and optimal pore sizes for binding C_2H_2.

In order to understand the C_2H_2 adsorption isotherms in these materials, we conducted detailed modeling studies by first-principles DFT-D (dispersion-corrected density-functional theory) calculations. In SIFSIX-1-Cu, C_2H_2 molecules are bound through strong C-H···F hydrogen (H) bonding (2.017 Å) and van der Waals (vdW) interactions with the 4,4'-bipyridine linkers (Fig. 1C and fig. S10) (*24*). The DFT-D calculated static adsorption energy ($\triangle E$) is 44.6 kJ/mol. Each unit cell of SIFSIX-1-Cu contains four equivalent exposed F atoms and each exposed F atom binds one C_2H_2 molecule. The distance between neighboring adsorbed C_2H_2 is ideal for them to synergistically interact with each other through multiple $H^{\delta+}\cdots C^{\delta-}$ dipole-dipole interactions (Fig. 1C), further enhancing the energy of adsorption. As four C_2H_2 molecules are adsorbed per unit cell, the $\triangle E$ of C_2H_2 increases to 47.0 kJ/mol. The strong binding of C_2H_2 at F atoms and the geometric arrangement of SiF_6^{2-} anions enables the efficient packing of four C_2H_2 molecules per unit cell and extraordinary C_2H_2 uptake at 298 K and 1 bar (about 4.4 C_2H_2 per unit cell).

In contrast, C_2H_2 adsorption is notably weaker in the wider pore material SIFSIX-2-Cu (10.5 Å by 10.5 Å cavity) versus that in SIFSIX-1-Cu ($\triangle E$: 34.6 vs. 44.6 kJ/mol; uptake: 5.3 vs. 8.5 mmol/g). The C-H···F H-bonding interaction from SiF_6^{2-} sites is of the same nature in these isoreticular networks (Fig. 1, C and D). However, vdW interaction between C_2H_2 and the organic linker in SIFSIX-2-Cu is weak compared to SIFSIX-1-Cu. We attribute this difference to the larger pore size and weaker vdW potential overlap (fig. S10 and S11) (*24*). Moreover, at high gas uptake, the C_2H_2 molecules adsorbed on adjacent F sites are too far separated to have synergistic guest-guest interactions. However, in the twofold interpenetrated structure of SIFSIX-2-Cu-i, one C_2H_2 molecule can be simultaneously bound by two F atoms from different nets through cooperative C-H···F H-bonding (2.013 and 2.015 Å, Fig. 1E), which enables the strongest energy of C_2H_2 binding ($\triangle E$: 52.9 kJ/mol) yet observed in SIFSIX materials. The strong adsorption energy of SIFSIX-2-Cu-i contributes to its extremely high uptake capacity at low pressure. In SIFSIX-3-Zn and SIFSIX-3-Ni, the strongest CO_2 adsorbents, the pore size is smallest and C_2H_2 molecules are primarily adsorbed at a different site in the 1D channel along the *c* axis (Fig. 1F, $\triangle E$: 50.3 kJ/mol). The secondary adsorption site in SIFSIX-3-Zn (fig. S12) (*24*) exhibits a much smaller adsorption energy (25.9 kJ/mol), which results in lower C_2H_2 uptake compared with that of SIFSIX-2-Cu-i.

The weakly basic SiF_6^{2-} (pK_a = 1.92) sites and their geometric disposition enables strong binding with weakly acidic C_2H_2 molecules. Because C_2H_2 is more acidic than C_2H_4 (pK_a: 25 vs. 44) (*17*) and the geometry is more optimal for C_2H_2 binding, there are much stronger interactions with C_2H_2 than C_2H_4 ($\triangle E$ in SIFSIX-1-Cu: 44.6 vs. 27.2 kJ/mol, SIFSIX-2-Cu-i: 52.9 vs. 39.8 kJ/mol). The calculated H-bond distances between C_2H_4 and SiF_6^{2-} sites are 2.541 and 2.186 Å in SIFSIX-1-Cu and SIFSIX-2-Cu-i, respectively, which are longer than those between C_2H_2 and SiF_6^{2-} sites (figs. S13 and S14) (*24*).

DFT-D was used to simulate C_2H_2 adsorption sites and high-resolution neutron powder diffraction data were collected on C_2D_2-loaded samples of SIFSIX-1-Cu·4C_2D_2 and SIFSIX-2-Cu-i·1.7C_2D_2 at 200 K to establish the structure of the C_2H_2 binding sites through Rietveld structural refinements (figs. S15 and S16) (*24*). Each unit cell of SIFSIX-1-Cu is filled with four C_2D_2 molecules that are arranged in an ordered planar structure (Fig. 1, G and H), consistent with the DFT-D modeling results. C-D···F H-bonding occurs between C_2D_2 and SiF_6^- anions (2.063 Å), and $D^{\delta+}\cdots C^{\delta-}$ distances between neighboring C_2D_2 molecules are 3.063 and 3.128 Å. In SIFSIX-2-Cu-i, each C_2H_2 interacts with two SiF_6^- anions via dual C-D···F H-bonding (2.134 Å, fig. S17) (*24*).

The separation of C_2H_2 from C_2H_4 is necessary for the production of high-purity C_2H_4 and C_2H_2. In the production of polymer-grade C_2H_4, removal of trace C_2H_2 (about 1%) from C_2H_4 gas must meet the requirement of < 40 parts per million (ppm) C_2H_2 in the downstream polymerization reaction (*17*). Similarly in the production of polymer-grade C_2H_2 by pyrolysis of coal and biomass, the capture of C_2H_2 from C_2H_2/C_2H_4 (90/10 to 50/50, v/v) is a crucial step. Existing methods, such as solvent absorption and partial hydrogenation of C_2H_2 (*25*) are energy intensive, so there is an urgent need to develop efficient porous materials for C_2H_2 capture from C_2H_4.

To address gas mixture separations, we first determined the C_2H_2/C_2H_4 separation selectivities of the SIFSIX materials with ideal adsorbed solution theory (IAST) calculations (*26*) (Fig. 2 and fig. S20) (*24*). SIFSIX-2-Cu-i exhibits record C_2H_2/C_2H_4 selectivities (39.7 to 44.8, Fig. 2A), even greater than that of M'MOF-3a (table S1). Because SIFSIX-2-Cu-i adsorbs a high amount of C_2H_2 under very low pressures,

SIFSIX-2-Cu-i not only has the highest C_2H_2/C_2H_4 selectivities (Fig. 2B) but also the highest C_2H_2 uptake (Fig. 2D) for C_2H_2/C_2H_4 (1/99) mixtures. SIFSIX-1-Cu exhibits moderately high C_2H_2/C_2H_4 separation selectivities (7.1-10.6), which are greater than those of FeMOF-74 (2.1) (*18*) and NOTT-300 (2.2-2.5) (*14*) (Fig. 2A). For C_2H_2/C_2H_4 (1/99) mixtures, SIFSIX-1-Cu exhibits greater selectivities (10.6) than SIFSIX-3-Zn (8.8), SIFSIX-3-Ni (5.0) (Fig. 2B). Its C_2H_2 uptake from the 1/99 mixture are the second highest of the compounds investigated (Fig. 2D). Given that SIFSIX-1-Cu exhibits a relatively high surface area, SIFSIX-1-Cu should also be very efficient for C_2H_2/C_2H_4 (1/99) separations. Notably, SIFSIX-1-Cu exhibits higher C_2H_2 uptakes than benchmark MOFs including FeMOF-74, NOTT-300 and UTSA-100a. Its high C_2H_2/C_2H_4 selectivities (Fig. 2A) make SIFSIX-1-Cu most suitable for C_2H_2/C_2H_4 (50/50) separation (Fig. 2C and fig. S20) (*24*). Some further comparisons with respect to how these MOFs perform with respect to C_2H_2/C_2H_4 separations are in table S1 (*24*).

Transient breakthrough simulations (*27*) were conducted in order to demonstrate C_2H_2/C_2H_4 separation performances of the SIFSIX materials in column adsorption processes. Two C_2H_2/C_2H mixtures (1/99 and 50/50) were used as feeds to mimic the industrial process conditions. Clean separations are realized with all five SIFSIX MOFs; C_2H_4 first eluted through the bed to afford a polymer-grade gas, then C_2H_2 broke through from the bed at a certain time of τ_{break} (Fig. 3A and figs. S21 and S22) (*24*). The dimensionless breakthrough times (τ_{break}) of C_2H_2 for SIFSIX-1-Cu (1/99 and 50/50 mixture) and SIFSIX-2-Cu-i (1/99 mixture) exceed the other SIFSIX materials and MOFs studied (Fig. 3, A and B). The amount of C_2H_2 captured in SIFSIX-1-Cu and SIFSIX-2-Cu-i from 1/99 mixture are up to 265.3 and 780.0 mmol/L, which compares favorably with state-of-art adsorbents such as UTSA-100a (135.5 mmol/L), FeMOF-74 (100.7 mmol/L) and NOTT-300 (68.3 mmol/L). SIFSIX-2-Cu-i efficiently removes trace C_2H_2 from C_2H_4 gas (1/99) whereas SIFSIX-1-Cu demonstrates excellent C_2H_2 capacity with an uptake of 5533 mmol/L from 50/50 mixture, ~ 37% greater than that of FeMOF-74 (Fig. 3F).

We further examined these materials in actual adsorption processes for both 1/99 and 50/50 mixtures through experimental breakthrough studies. Highly efficient separations for C_2H_2/C_2H_4 mixtures were indeed realized (Fig. 3, D and E). For the capture of C_2H_2 from the 1/99 mixture, the concentration of C_2H_2 in the gas exiting the adsorber for up to 140 min was measured to be below 2 ppm and the purity of C_2H_4 was > 99.998% (fig. S23) (*24*). The hierarchy of breakthrough time for the 1/99 mixture was SIFSIX-2-Cu-i > SIFSIX-1-Cu > SIFSIX-3-Zn, and for the 50/50 mixture was SIFSIX-1-Cu > SIFSIX-3-Zn > SIFSIX-2-Cu-i (Fig. 3, D and E). These experiments are consistent with simulated breakthrough results. Although the uptake of C_2H_2 on SIFSIX-3-Zn at low pressure for the 1/99 mixture is higher than that of SIFSIX-1-Cu (Fig. 1B), SIFSIX-1-Cu exhibits longer breakthrough time for C_2H_2, presumably because of its higher selectivity (Fig. 2B). The amounts of C_2H_2 captured by SIFSIX-1-Cu, SIFSIX-2-Cu-i, and SIFSIX-3-Zn from the 1/99 mixture during the breakthrough process are 0.38, 0.73 and 0.08 mmol/g, and that from the 50/50 mixture are 6.37, 2.88 and 1.52 mmol/g, respectively, are also in excellent agreement with the simulated results except for SIFSIX-3-Zn (tables S12 and S13) (*24*).

In the production process of high-purity C_2H_4, the feed gases for the unit of C_2H_2 removal are contaminated with trace levels of CO_2 (< 50 ppm), H_2O (< 5 ppm), and O_2 (< 5 ppm). We conducted breakthrough experiments for the 1/99 mixture using SIFSIX-2-Cu-i, the best performing material for capture of trace amounts of C_2H_2. These experiments indicate that the presence CO_2 has only slight (1000 ppm CO_2) or no (10 ppm CO_2) effect on the separation of C_2H_2 from C_2H_4 (fig. S24) (*24*). Moisture (6 to 1340 ppm) and oxygen (2200 ppm) do not affect the C_2H_2 capture ability of SIFSIX-2-Cu-i (figs. S25 and S26) (*24*). Breakthrough performance of SIFSIX-2-Cu-i and SIFSIX-3-Zn for 1/99 mixture was not observed to decline during 16 and 3 cycles, respectively (figs. S28 and S29) (*24*), and the SIFSIX materials retain their stability after breakthrough experiments (figs. S1 and S30) (*24*).

The SIFSIX materials studied herein were found to exhibit excellent C_2H_2 storage performance. The volumetric uptake of C_2H_2 in SIFSIX-1-Cu at 298 K and 1.0 bar is the highest (0.191 g/cm^3) among these SIFSIX materials (table S14) (*24*). The storage C_2H_2 densities in the pores of SIFSIX-1-Cu, SIFSIX-2-Cu-i and SIFSIX-3-Zn at 298 K are 0.388, 0.403 and 0.499 g/cm^3, respectively.

The basic principles outlined here are likely to be applicable to other gas mixtures. Primary binding sites will be necessary to initiate their recognition for specific gas molecules while suitable pore sizes and spacing will enforce synergistic binding to multiple sites including through intermolecular guest-guest interactions to form the so-called "gas clusters". This work not only reveals a path forward for industrial C_2H_2/C_2H_4 separations, but also facilitates a design or crystal engineering approach to the development of porous materials for other gas separations.

REFERENCES AND NOTES

1. S. Kitagawa, Porous materials and the age of gas. *Angew. Chem. Int. Ed.* **54**, 10686–10687 (2015). Medline doi:10.1002/anie.201503835
2. R. Vaidhyanathan, S. S. Iremonger, G. K. Shimizu, P. G. Boyd, S. Alavi, T. K. Woo, Direct observation and quantification of CO_2 binding within an amine-functionalized nanoporous solid. *Science* **330**, 650–653 (2010). Medline doi:10.1126/science.1194237
3. N. T. T. Nguyen, H. Furukawa, F. Gándara, H. T. Nguyen, K. E. Cordova, O. M. Yaghi, Selective capture of carbon dioxide under humid conditions by hydrophobic chabazite-type zeolitic imidazolate frameworks. *Angew. Chem. Int. Ed.* **53**,

10645–10648 (2014). Medline doi:10.1002/ange.201403980
4. N. L. Rosi, J. Eckert, M. Eddaoudi, D. T. Vodak, J. Kim, M. O'Keeffe, O. M. Yaghi, Hydrogen storage in microporous metal-organic frameworks. *Science* **300**, 1127–1129 (2003). Medline doi:10.1126/science.1083440
5. Y. Peng, V. Krungleviciute, I. Eryazici, J. T. Hupp, O. K. Farha, T. Yildirim, Methane storage in metal-organic frameworks: Current records, surprise findings, and challenges. *J. Am. Chem. Soc.* **135**, 11887–11894 (2013). Medline doi:10.1021/ja4045289
6. J. A. Mason, J. Oktawiec, M. K. Taylor, M. R. Hudson, J. Rodriguez, J. E. Bachman, M. I. Gonzalez, A. Cervellino, A. Guagliardi, C. M. Brown, P. L. Llewellyn, N. Masciocchi, J. R. Long, Methane storage in flexible metal-organic frameworks with intrinsic thermal management. *Nature* **527**, 357–361 (2015). Medline doi:10.1038/nature15732
7. S. Ma, D. Sun, J. M. Simmons, C. D. Collier, D. Yuan, H. C. Zhou, Metal-organic framework from an anthracene derivative containing nanoscopic cages exhibiting high methane uptake. *J. Am. Chem. Soc.* **130**, 1012–1016 (2008). Medline doi:10.1021/ja0771639
8. H. Furukawa, K. E. Cordova, M. O'Keeffe, O. M. Yaghi, The chemistry and applications of metal-organic frameworks. *Science* **341**, 1230444 (2013). Medline
9. S. J. Datta, C. Khumnoon, Z. H. Lee, W. K. Moon, S. Docao, T. H. Nguyen, I. C. Hwang, D. Moon, P. Oleynikov, O. Terasaki, K. B. Yoon, CO_2 capture from humid flue gases and humid atmosphere using a microporous coppersilicate. *Science* **350**, 302–306 (2015). Medline doi:10.1126/science.aab1680
10. Z. J. Zhang, Z.-Z. Yao, S. Xiang, B. Chen, Perspective of microporous metal–organic frameworks for CO_2 capture and separation. *Energy Environ. Sci.* **7**, 2868–2899 (2014). doi:10.1039/C4EE00143E
11. Q. Lin, T. Wu, S. T. Zheng, X. Bu, P. Feng, Single-walled polytetrazolate metal-organic channels with high density of open nitrogen-donor sites and gas uptake. *J. Am. Chem. Soc.* **134**, 784–787 (2012). Medline doi:10.1021/ja2092882
12. J.-R. Li, R. J. Kuppler, H.-C. Zhou, Selective gas adsorption and separation in metal-organic frameworks. *Chem. Soc. Rev.* **38**, 1477–1504 (2009). Medline doi:10.1039/b802426j
13. R. Matsuda, R. Kitaura, S. Kitagawa, Y. Kubota, R. V. Belosludov, T. C. Kobayashi, H. Sakamoto, T. Chiba, M. Takata, Y. Kawazoe, Y. Mita, Highly controlled acetylene accommodation in a metal-organic microporous material. *Nature* **436**, 238–241 (2005). Medline doi:10.1038/nature03852
14. S. Yang, A. J. Ramirez-Cuesta, R. Newby, V. Garcia-Sakai, P. Manuel, S. K. Callear, S. I. Campbell, C. C. Tang, M. Schröder, Supramolecular binding and separation of hydrocarbons within a functionalized porous metal-organic framework. *Nat. Chem.* **7**, 121–129 (2014). Medline doi:10.1038/nchem.2114
15. H. Wu, Q. Gong, D. H. Olson, J. Li, Commensurate adsorption of hydrocarbons and alcohols in microporous metal organic frameworks. *Chem. Rev.* **112**, 836–868 (2012). Medline doi:10.1021/cr200216x
16. J.-P. Zhang, X.-M. Chen, Optimized acetylene/carbon dioxide sorption in a dynamic porous crystal. *J. Am. Chem. Soc.* **131**, 5516–5521 (2009). Medline doi:10.1021/ja8089872
17. T. L. Hu, H. Wang, B. Li, R. Krishna, H. Wu, W. Zhou, Y. Zhao, Y. Han, X. Wang, W. Zhu, Z. Yao, S. Xiang, B. Chen, Microporous metal-organic framework with dual functionalities for highly efficient removal of acetylene from ethylene/acetylene mixtures. *Nat. Commun.* **6**, 7328–7335 (2015). Medline doi:10.1038/ncomms8328
18. E. D. Bloch, W. L. Queen, R. Krishna, J. M. Zadrozny, C. M. Brown, J. R. Long, Hydrocarbon separations in a metal-organic framework with open iron(II) coordination sites. *Science* **335**, 1606–1610 (2012). Medline doi:10.1126/science.1217544
19. M. C. Das, Q. Guo, Y. He, J. Kim, C. G. Zhao, K. Hong, S. Xiang, Z. Zhang, K. M. Thomas, R. Krishna, B. Chen, Interplay of metalloligand and organic ligand to tune micropores within isostructural mixed-metal organic frameworks (M'MOFs) for their highly selective separation of chiral and achiral small molecules. *J. Am. Chem. Soc.* **134**, 8703–8710 (2012). Medline doi:10.1021/ja302380x
20. P. Nugent, Y. Belmabkhout, S. D. Burd, A. J. Cairns, R. Luebke, K. Forrest, T. Pham, S. Ma, B. Space, L. Wojtas, M. Eddaoudi, M. J. Zaworotko, Porous materials with optimal adsorption thermodynamics and kinetics for CO_2 separation. *Nature* **495**, 80–84 (2013). Medline doi:10.1038/nature11893
21. S. Noro, R. Kitaura, M. Kondo, S. Kitagawa, T. Ishii, H. Matsuzaka, M. Yamashita, Framework engineering by anions and porous functionalities of Cu(II)/4,4′-bpy coordination polymers. *J. Am. Chem. Soc.* **124**, 2568–2583 (2002). Medline doi:10.1021/ja0113192
22. O. Shekhah, Y. Belmabkhout, Z. Chen, V. Guillerm, A. Cairns, K. Adil, M. Eddaoudi, Made-to-order metal-organic frameworks for trace carbon dioxide removal and air capture. *Nat. Commun.* **5**, 4228–4234 (2014). Medline doi:10.1038/ncomms5228
23. A. Kumar, D. G. Madden, M. Lusi, K.-J. Chen, E. A. Daniels, T. Curtin, J. J. Perry 4th, M. J. Zaworotko, Direct air capture of CO_2 by physisorbent materials. *Angew. Chem. Int. Ed.* **54**, 14372–14377 (2015). doi:10.1002/anie.201506952 Medline
24. Materials and methods are available as supplementary materials on *Science* Online.
25. F. Studt, F. Abild-Pedersen, T. Bligaard, R. Z. Sørensen, C. H. Christensen, J. K. Nørskov, Identification of non-precious metal alloy catalysts for selective hydrogenation of acetylene. *Science* **320**, 1320–1322 (2008). Medline doi:10.1126/science.1156660
26. K. S. Walton, D. S. Sholl, Predicting multicomponent adsorption: 50 years of the ideal adsorbed solution theory. *AIChE J.* **61**, 2757–2762 (2015). doi:10.1002/aic.14878
27. R. Krishna, Methodologies for evaluation of metal–organic frameworks in separation applications. *RSC Adv.* **5**, 52269–52295 (2015). doi:10.1039/C5RA07830J
28. K. M. Sundaram, M. M. Shreehan, E. F. Olszewski, "Ethylene," in *Kirk-Othmer Encyclopedia of Chemical Technology* (Wiley Online Library, 2001).
29. A. C. Larson, R. B. Von Dreele, *General Structure Analysis System* (LAUR 86-748, Los Alamos National Laboratory, 1994).
30. V. Barone, M. Casarin, D. Forrer, M. Pavone, M. Sambi, A. Vittadini, Role and effective treatment of dispersive forces in materials: Polyethylene and graphite crystals as test cases. *Comput. Chem.* **30**, 934–939 (2009). Medline doi:10.1002/jcc.21112
31. R. T. Yang, *Gas Separation by Adsorption Processes* (Butterworth Publishers, 1986).
32. Y.-B. He, R. Krishna, B. Chen, Metal-organic frameworks with potential for energy-efficient adsorptive separation of light hydrocarbons. *Energy Environ. Sci.* **10**, 9107–9120 (2012). doi:10.1039/c2ee22858k
33. R. Krishna, The Maxwell-Stefan description of mixture diffusion in nanoporous crystalline materials. *Microporous Mesoporous Mater.* **185**, 30–50 (2014). doi:10.1016/j.micromeso.2013.10.026
34. S. D. Burd, S. Ma, J. A. Perman, B. J. Sikora, R. Q. Snurr, P. K. Thallapally, J. Tian, L. Wojtas, M. J. Zaworotko, Highly selective carbon dioxide uptake by [Cu(bpy-*n*)$_2$(SiF$_6$)] (bpy-1 = 4,4′-bipyridine; bpy-2 = 1,2-bis(4-pyridyl)ethene). *J. Am. Chem. Soc.* **134**, 3663–3666 (2012). Medline doi:10.1021/ja211340t

ACKNOWLEDGMENTS

This work is supported by the National Natural Science Foundation of China (21222601, 21436010 and 21476192), Zhejiang Provincial Natural Science Foundation of China (LR13B060001), Ten Thousand Talent Program of China (H.X.), Welch Foundation (AX-1730), KAUST for the Competitive Research Funds (URF/1/1672-01-01), the Science Foundation Ireland (M.Z., SFI Award 13/RP/B2549). We thank T.L.H., Y.F.Z., W.D.S., and M.D.J. for their help and arrangement of the breakthrough experiments, A.K. for the help in sample characterization, and Z.G.Z. and B.G.S. for their experimental discussions. Metrical data for the solid-state structures of SIFSIX-2-Cu-i·C_2D_2 and SIFSIX-1-Cu·C_2D_2 are available free of charge from the Cambridge Crystallographic Data Centre under reference numbers CCDC 1471795 and 1471796. The authors and their affiliations have filed a patent application on the results presented herein.

SUPPLEMENTARY MATERIALS

www.sciencemag.org/cgi/content/full/science.aaf2458/DC1
Materials and Methods
Figs. S1 to S32
Tables S1 to S15
References (*28*–*34*)

12 January 2016; accepted 5 May 2016
Published online 19 May 2016
10.1126/science.aaf2458

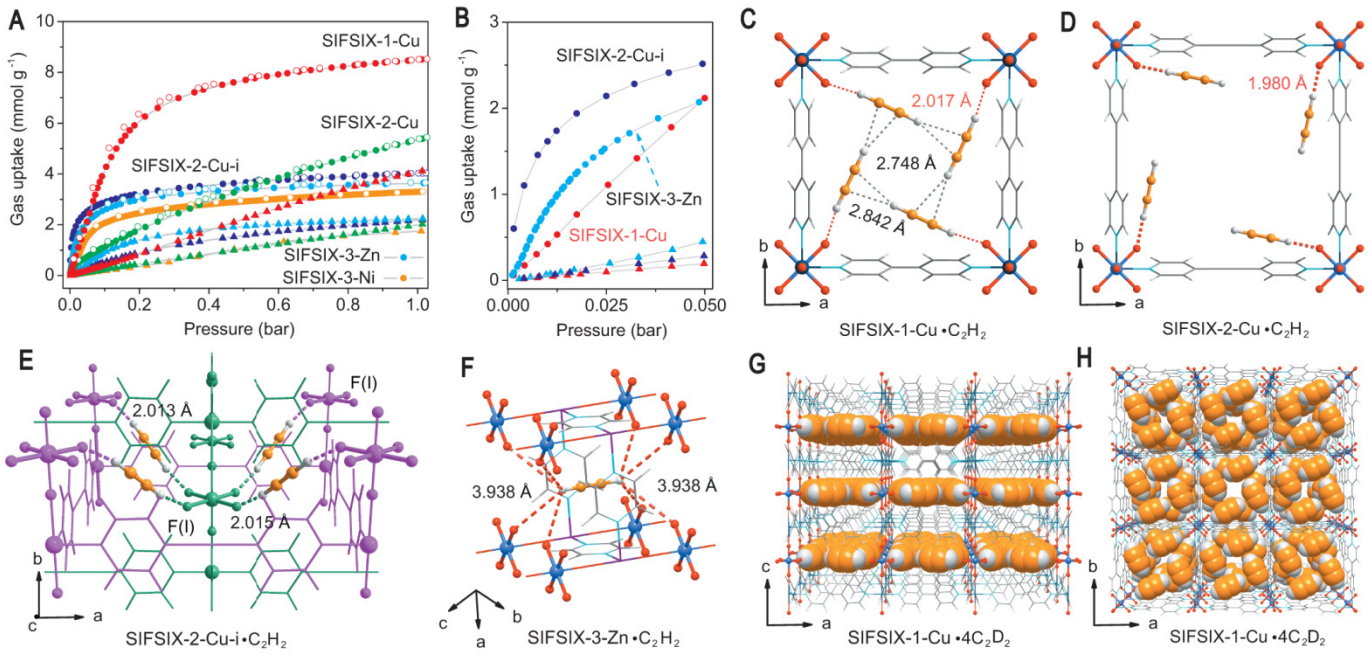

Fig. 1. C_2H_2 and C_2H_4 adsorption isotherms and DFT-D simulated optimized C_2H_2 adsorption sites of the MOFs, and neutron crystal structure of SIFSIX-1-Cu·4C_2D_2. (**A** and **B**) Adsorption isotherms of C_2H_2 (circle) and C_2H_4 (triangle) in SIFSIX-1-Cu, SIFSIX-2-Cu, SIFSIX-2-Cu-i, SIFSIX-3-Zn, and SIFSIX-3-Ni in two pressure regions, 0-1.0 bar (**A**) and 0-0.05 bar (B) at 298 K. (**C** to **F**) DFT-D calculated C_2H_2 adsorption binding sites in SIFSIX-1-Cu (C), SIFSIX-2-Cu (D), SIFSIX-2-Cu-i (E), the different nets are highlighted in pink and green color for clarity, and SIFSIX-3-Zn (F). Color code: F, red; Si, light blue; C, gray-50%; H, gray-25%; N, sky blue; Cu, dark teal; Zn, violet. (**G** and **H**) Neutron crystal structure of SIFSIX-1-Cu·4C_2D_2 at 200 K from Rietveld analysis.

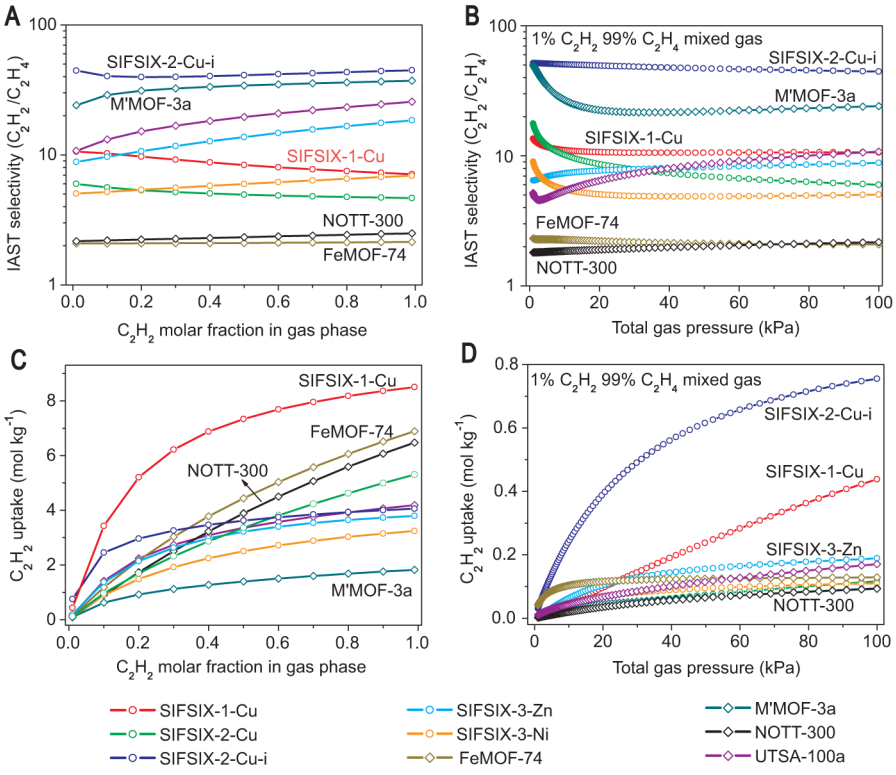

Fig. 2. IAST calculations for C_2H_2/C_2H_4 mixtures on the MOFs. **(A** and **B)** Comparison of IAST selectivities of SIFSIX materials and previously reported best-performing materials for C_2H_2/C_2H_4 mixtures with varying C_2H_2 molar fraction at 100 kPa (A) and a C_2H_2/C_2H_4 mixture containing 1% C_2H_2 (B). **(C** and **D)** Uptake capacity of C_2H_2 on MOFs from C_2H_2/C_2H_4 mixtures with varying C_2H_2 molar fraction at 100 kPa (C) and C_2H_2/C_2H_4 mixture containing 1% C_2H_2 (D).

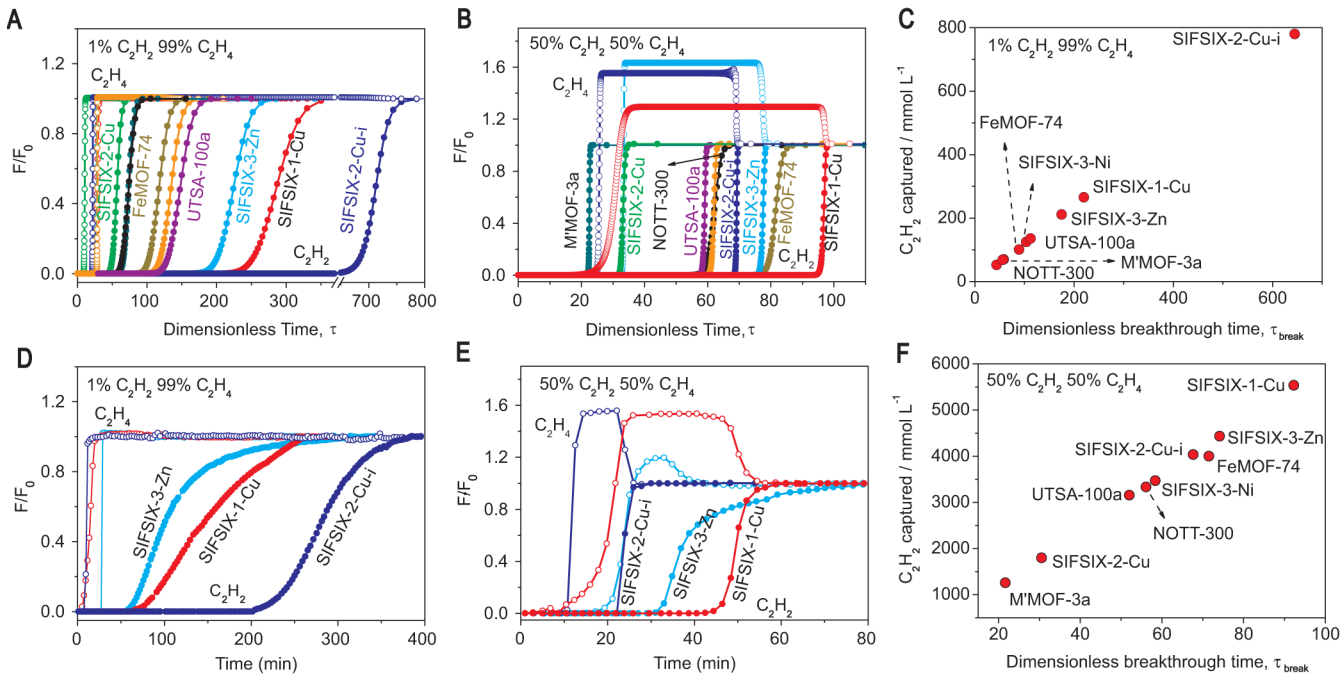

Fig. 3. Simulated and experimental column breakthrough results. (**A** and **B**) Simulated column breakthrough curves for C_2H_2/C_2H_4 separations (1/99) (A) and (50/50) (B) with SIFSIX materials and previously reported best-performing materials. (**C** and **F**) Plots of the amount of C_2H_2 captured as a function of τ_{break} in the simulated column breakthrough for C_2H_2/C_2H_4 separations (1/99) (C) and (50/50) (F). (**D** and **E**) Experimental column breakthrough curves for C_2H_2/C_2H_4 separations (1/99) (D) and (50/50) (E) with SIFSIX-1-Cu, SIFSIX-2-Cu, and SIFSIX-3-Zn at 298 K and 1 atm.

Pore chemistry and size control in hybrid porous materials for acetylene capture from ethylene

Xili Cui, Kaijie Chen, Huabin Xing, Qiwei Yang, Rajamani Krishna, Zongbi Bao, Hui Wu, Wei Zhou, Xinglong Dong, Yu Han, Bin Li, Qilong Ren, Michael J. Zaworotko and Banglin Chen (May 19, 2016)
published online May 19, 2016

Editor's Summary

Science (print ISSN 0036-8075; online ISSN 1095-9203) is published weekly, except the last week in December, by the American Association for the Advancement of Science, 1200 New York Avenue NW, Washington, DC 20005.